Micro-Homogeneous Charge Compression Ignition (HCCI) Combustion: Investigations Employing Detailed Chemical Kinetic Modeling and Experiments

H. T. Aichlmayr haich@me.umn.edu (612) 626-1878
D. B. Kittelson kitte001@umn.edu (612) 625-1808
M. R. Zachariah mrz@me.umn.edu (612) 626-9081

Departments of Mechanical Engineering and Chemistry and
the Minnesota Supercomputing Institute
The University of Minnesota
111 Church St. SE, Minneapolis, MN 55455 USA

Abstract

This paper describes work done at the University of Minnesota and Honeywell International in support of the MEMS Free-Piston Knock Engine Program; overall sponsorship is provided by the Defense Advanced Research Projects Agency (DARPA). This program is one of four efforts underway to develop micro-engines for power generation. In addition to materials and manufacturing concerns, combustion within sub-quenching distance spaces, or micro-combustion, is a key concern. This paper presents experimental and computational evidence that Homogeneous Charge Compression Ignition (HCCI) combustion is a viable micro-engine combustion scheme.

Introduction

Under the auspices of the Defense Advanced Research Projects Agency (DARPA), several micro-engine development programs are underway. These include the Micro-Gas Turbine Engine at the Massachusetts Institute of Technology [1], the MEMS Rotary Engine at The University of California Berkeley [2], the MEMS Free-Piston Knock Engine at Honeywell International [3, 4], and the MEMS Free-Piston Engine-Generator at the Georgia Institute of Technology [5]. The common motivation for these programs is to replace batteries in various applications with integrated packages comprised of an engine-generator, control unit, and fuel tank. In principle, these units could deliver between 10 and 20 watts of electricity from packaged volumes as small as $1\,\mathrm{cm}^3$.

Micro-Engines

The rationale for developing micro-engines is rooted in energy density: Hydrocarbon fuels such as propane, have a lower heating value of approximately $46\,\frac{\mathrm{MJ}}{\mathrm{kg}}$. Batteries on the other hand, have energy densities of $1\,\frac{\mathrm{MJ}}{\mathrm{kg}}$ at most [3]. Consequently an engine-generator would only need to have an overall fuel conversion efficiency of 2.5% to surpass any battery. Of note, the overall fuel conversion efficiency of the smallest mass-produced model airplane engine ($0.16\,\mathrm{cm}^3$ displacement) is approximately 4% [6]. Consequently this proposition is realistic.

Developing a micro-engine however, is not a trivial affair. Materials and fabrication requirements for instance, pose particularly daunting challenges. Moreover, small characteristic dimensions imply that the combustion and gas exchange processes must be conducted in physical regimes entirely different from conventional, i.e., large-scale, engines. Consequently simply scaling-down existing engine designs and their associated combustion modes, e.g., spark ignition, is not possible. This paper addresses the problem of small-scale engine combustion. Curiously, when compared to other technical challenges, micro-HCCI combustion appears to pose few difficulties.

Micro-Combustion

Micro-combustion is defined here to be combustion that occurs in spaces whose open dimensions are equivalent to, or smaller than, typical flame quenching distances. Flame quenching occurs when thermal energy is transfered to the boundaries faster than it can be liberated by exothermic chemical reactions. In general, this is a significant effect in small dimensions because the specific heat transfer rate given by

$$\dot{q} = \frac{\dot{Q}}{m} = \frac{\int_{\mathrm{A_s}} \dot{q}'' dA}{\int_{\tilde{\mathrm{V}}} \rho dV} = \frac{\bar{\dot{q}}''}{\bar{\rho}} \left(\frac{\mathrm{A_s}}{\tilde{\mathrm{V}}} \right), \tag{1}$$

increases with the surface-area-to-volume ratio denoted by $\frac{\mathrm{A_s}}{\tilde{\mathrm{V}}}$.

Flame quenching is a fundamental limitation with which all micro-internal combustion engine programs must cope. Consequently each effort may be characterized according to the manner in which it is addressed: Waitz et al. [7] exploit the wide flammability limits of hydrogen and plan to burn hydrocarbons with the assistance of a catalyst., Fernandez-Pello et al. [2] elevate wall temperatures to yield an essentially adiabatic engine., Allen et al. [5] spark-ignite the charge in multiple locations., and Yang et al. [3, 4] employ "Knock," or Homogeneous Charge Compression Ignition (HCCI) combustion.

Homogeneous Charge Compression Ignition Combustion

HCCI is an alternative engine combustion mode first identified by Onishi et al. [8]. It entails compressing a fuel-air mixture until it explodes. Consequently it is intimately linked to chemical kinetics and the compression process [9]. It should be noted that although HCCI shares features with Diesel and spark ignition (SI) combustion, it is fundamentally different. Experimentally verified [10, 11, 12] features of HCCI include: 1. Ignition occurs simultaneously at numerous locations within the combustion chamber., 2. Traditional flame propagation is absent., 3. The charge is consumed very rapidly., 4. Ignition is not initiated by an external event., 5. Extremely lean mixtures may be ignited., and 6. A wide variety of fuels may be used.

HCCI is also called "knock combustion" because it is closely related to engine knock, i.e., the phenomenon that occurs in an SI engine when a pocket of fresh charge explodes before being consumed by an advancing flame front. HCCI however, does not damage engine components because very lean mixtures are employed and the explosion is essentially homogeneous. Hence a non-uniform pressure rise and subsequent shock wave generation does not occur.

Currently, several research and development efforts are underway to adapt conventional engines to HCCI. This interest is mostly a result of HCCI being able to largely eliminate the primary vices of Diesel engines: NO_x and particulate emissions. These benefits are attributable to employing extraordinarily lean homogeneous mixtures. Moreover, an added benefit is that fuel economy comparable to a Diesel engine [13] is possible.

Despite many contributions toward the understanding of HCCI [9, 13, 14, 15, 16, 17, 18, 19, 20, 21, 22, 23, 24, 25, 26], it is presently impractical. Unfortunately, the use of auto-ignition results in an inability to directly synchronize ignition and the piston motion, i.e., timing. This is in contrast to SI and Diesel engines where direct ignition control is achieved via spark and injection timing. Instead, only indirect methods may be used to control HCCI. Examples of these methods include preheating the fresh charge, multiple fuels, variable compression ratio, water injection, and variable exhaust gas recirculation (EGR).

Understandably, these methods are generally very complicated. Hence a great deal of computational and experimental work is directed toward devising and evaluating them.

In the context of micro-engines however, the most significant aspect of HCCI is that it is possible to burn the fresh charge essentially without flame propagation. Consequently the flame quenching problem is circumvented in a simple manner. Further, HCCI is essentially limited by kinetics. Therefore HCCI engine operating speeds may easily exceed those of engines employing conventional combustion. This is a crucial result because for an engine to maintain a constant power output, operating speeds must increase when characteristic dimensions are reduced [27].

Modeling Micro-HCCI

In light of the dual benefits that HCCI offers micro-engine designers, one is immediately led to ask, "How small can an engine be?" Aichlmayr et al. [28] attempted to answer this question by combining detailed chemical kinetic modeling, a diffusion-based heat transfer model, and performance estimation to determine plausible micro-engine designs. Of note, detailed homogeneous gas-phase kinetics are the generally-accepted means to predict ignition [29]. Also, it should be emphasized that slider-crank piston motion was assumed and that ignition timing was not considered.

The analysis was conducted as follows: First, an engine "design" is assumed to comprise a stroke to bore aspect ratio R, a compression ratio r, and a total cylinder volume V_t. Next, these designs were consolidated into two-dimensional maps corresponding to a set of charge initial conditions and specified power output. Finally, the designs were classified "possible" or "impossible" depending upon whether or not the charge would ignite. The classification was conducted using a modified version of SENKIN [30] and a butane mechanisim consisting of 394 species and 1909 reactions.

Operational maps were devised for power outputs of 10 W, 1 W, and 0.1 W. The key result is that the minimum engine size is primarily limited by heat transfer. To illustrate, operational maps for 1 W engines are presented in Figure 1. A comparison of Figure 1(a) and Figure 1(b) reveals that the region of operation

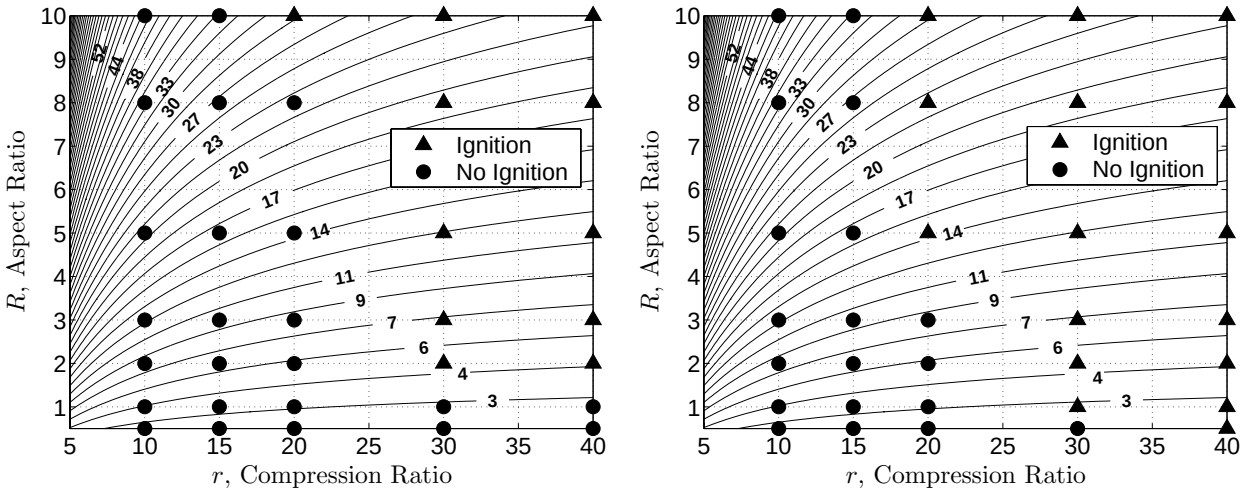

(a) Non-adiabatic engine.

(b) Adiabatic engine.

Figure 1. Operational map for a 1 W miniature HCCI engine operating with propane and air, Φ=0.5; initial conditions of 500 K and 1 atm and a wall temperature of 300 K are assumed. Contours indicate V_t in mm^3.

is reduced by heat transfer. Specifically, the designs with R<10 and r=20 are rendered impossible by heat transfer. Similar analyses conducted with the power output constrained to be 10 W and 0.1 W reveal that heat transfer becomes an increasingly significant limitation when the engine characteristic dimension

decreases—a result consistent with Eq. (1). Nonetheless, it is important to note that HCCI is predicted to be generally compatible with micro-engine operating conditions.

Free-Piston Versus Slider-Crank Motion

Although micro-engines and HCCI are apparently a good match, ignition timing remains a serious problem. A strategy which may lessen it is to employ a free-piston configuration [31, 32, 33]. A representative[1] free-piston engine configuration[2] is depicted in Figure 2(a). An engine of this type has essentially one moving part: A mechanically unconstrained piston. In contrast to a slider-crank arrangement, reciprocating motion

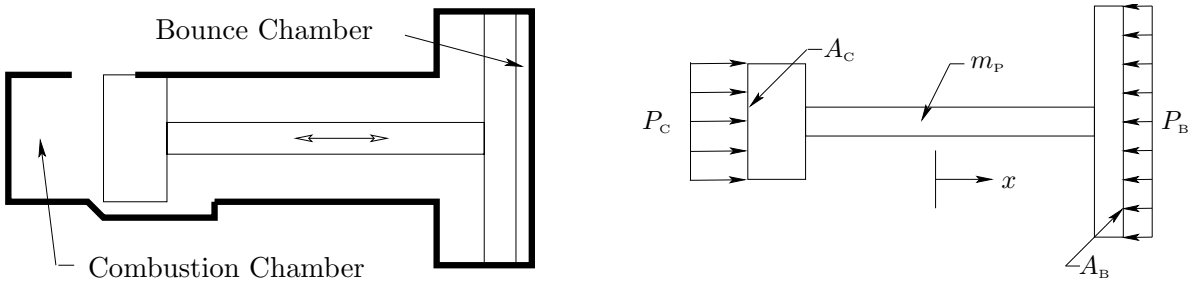

(a) Basic Free-Piston Engine

(b) Free-Piston Free-Body Diagram

Figure 2. The free-piston configuration.

is a result of a "thermodynamic-dynamic balance." To demonstrate, a free-body diagram of the piston is given in Figure 2(b); a force balance yields

$$\Sigma F_x = m_{\text{P}} \frac{d^2x}{dt^2} = P_{\text{C}} A_{\text{C}} - P_{\text{B}} A_{\text{B}}, \tag{2}$$

where m_{P}, P_{C}, and P_{B} are the piston mass and the combustion and bounce chamber pressures, respectively. Consequently the piston motion and the states of the gases occupying the combustion and bounce chambers are explicitly coupled.

Employing a free-piston in lieu of a crankshaft has significant ramifications. First, the compression ratio becomes an *operating* rather than a *design* parameter. This results in a simple yet effective means to moderate HCCI. Second, the operating speed is determined by the piston mass and the bounce chamber pressure. Consequently free-piston engines are nominally constant-speed machines. Finally, the piston kinematics (Figure 3(a)), and hence the temperature-pressure history of the fresh charge differ for free-piston and slider-crank arrangements. This fact may be readily discerned from Figure 3(b) where it should be recognized that for a perfect gas undergoing an isentropic compression, the temperature and pressure scale with the $\gamma - 1$ and γ powers of the compression ratio. Hence ignition in free-piston and slider-crank configurations are expected to proceed in different ways. It is therefore necessary to combine detailed chemical kinetics and a force balance such as Eq. (2), to investigate the interaction between HCCI and a free-piston. This task is incomplete at present.

Micro-HCCI Experiments

According to the numerical model, HCCI is a viable micro-engine combustion scheme. Of course, this result has little meaning unless it can be verified experimentally. Consequently a somewhat parallel experimental effort is underway at Honeywell Laboratories. Due to difficulties related to optimizing a two-stroke

[1] Consult Achten [34] for other free-piston engine configurations.

[2] Note that a counterbalancing mechanism, work extraction scheme, and a scavenging pump are omitted for clarity of the figure and brevity of the discussion.

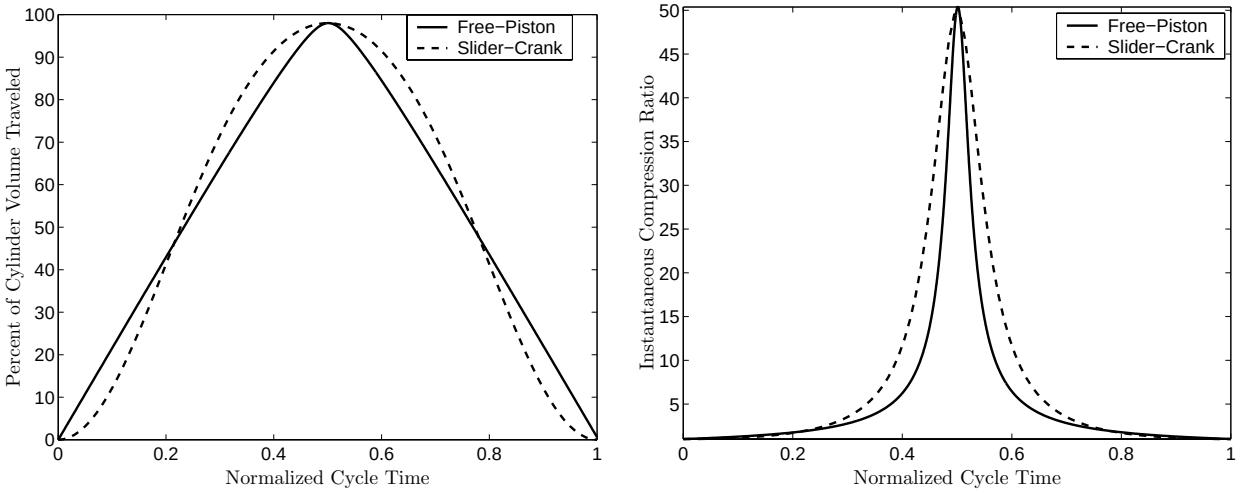

(a) Piston Position

(b) Compression Ratio

Figure 3. Free-piston and slider-crank motion comparison; both cases assume reversible adiabatic compression of a perfect gas.

gas exchange process, these experiments are of the "single-shot" variety and therefore represent a single compression-expansion event. Despite this limitation, these experiments have provided a wealth of physical insight with regard to free-piston dynamics and micro-HCCI combustion.

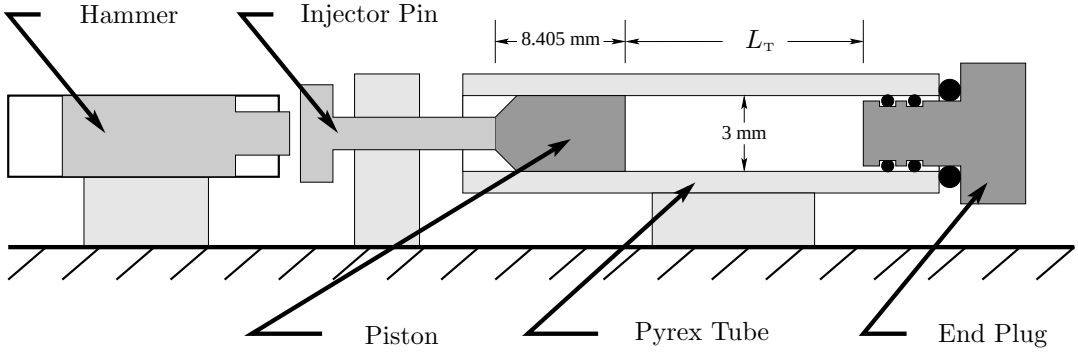

Figure 4. Single-Shot Experimental Setup

Experiment Setup and Procedure

The principle of the single-shot experiment is to drive a piston into a plugged cylinder filled with a combustible mixture. Referring to Figure 4, the piston and cylinder consist of a machined steel gauge pin and a Pyrex tube. The tubes have a nominal inside diameter of 3 mm, but they are selected such that the clearance between the piston and tube wall is approximately 5 μm. Also, the length of the tube determines the initial distance between the piston face and the end plug, L_T. These lengths have ranged from approximately 25 mm to 57 mm. The piston has an overall length of 8.405 mm and a mass of 0.435 g. In addition, the piston is neither lubricated nor does it make a gas-tight seal with the tube wall. End sealing of the cylinder is provided by a removable plug and three O-rings. The hammer and injector pin are used to generate and transfer linear momentum to the piston. Lastly, compressed air provides the initial impulse to the hammer and its release is initiated by a solenoid-actuated valve.

Not shown in Figure 4 however, is a Vision Research Phantom v4.0 digital camera. The camera is used to record the piston motion. Time-resolved measurements of piston velocity and position are then obtained from the movies. The maximum exposure and sampling rates of the camera are $100,000\,\frac{\text{frames}}{\text{s}}$ and $62,500\,\frac{\text{Pixels}}{\text{s}}$, respectively. These yield a maximum temporal resolution of $16\,\frac{\mu\text{s}}{\text{Frame}}$; all experiments are conducted at this setting. The distance resolution on the other hand, varies from 0.1 mm to 0.4 mm, depending upon the position of the camera. Lastly, acquisition is triggered by the actuating the compressed-air valve.

Currently, only mixtures of n-heptane and air have been investigated. Mixture preparation consists of drawing a fuel-air mixture from a bubbler into a syringe. To vary the charge equivalence ratio, the contents of the syringe are partially expelled and replaced with room air. Using this technique, it is possible to obtain equivalence ratios that are estimated to range from 0.25 to 2.9.

The single-shot experiment proceeds as follows: First, the end plug is removed and the hammer, injector pin, and piston are returned to their "ready" positions. Additionally, the camera is switched to "acquisition" mode. Next, a fuel-air mixture is prepared and injected into the cylinder. The end plug is inserted immediately afterward. The experiment commences with actuation of the compressed air valve. Shortly afterward, the hammer accelerates and strikes the injector pin. The injector pin subsequently impacts the piston and transfers the combined momentum of the hammer and injector pin to the piston before stopping. Of note, the combined mass of the hammer and injector pin are much greater than the piston. Consequently the post-impulse piston velocities can be as high as $40\,\frac{\text{m}}{\text{s}}$. The piston then proceeds to compress the charge and if conditions are right, an explosion occurs close to the end plug. Finally, the piston reverses direction and stops near the injector-pin end of the tube following several of impact-rebound events.

Experimental Results

The primary objective of the single-shot experiments is to verify that HCCI can occur in small volumes. To this end, images of the piston near the end of the compression stroke are pertinent. A sample image sequence is presented in Figure 5. In this case, the equivalence ratio is estimated to be 0.69 and HCCI combustion is clearly indicated by the optical emission appearing between the piston and the end plug. It should be noted however, that the Pyrex tube and the intensity of the flash obscure the fact that the piston is essentially stationary during most of the combustion event. Additionally, the incoming and outgoing velocities are $40\,\frac{\text{m}}{\text{s}}$ and $50\,\frac{\text{m}}{\text{s}}$, respectively. Consequently the piston experiences a net gain in kinetic energy.

Although the intensity of the optical emission in Figure 5 is impressive, these images are remarkable because they clearly demonstrate that combustion within a space approximately 3 mm in diameter and 0.3 mm wide is possible. Even more remarkable is the fact the charge was initially at ambient conditions, i.e., room temperature and 1 atm. Hence micro-combustion with a heavy hydrocarbon was achieved without having to employ catalysts, an ignition system, or external heating.

Further, a hallmark of HCCI is the ability to burn extremely lean mixtures. A logical question to ask would be: "Does this hold for micro-combustion?" According to Figure 6, it does. In this instance, the equivalence ratio is approximately 0.25. The combustion however, is noticeably weaker. Consequently HCCI does have a "lean limit," but it is important to recognize that it implies vanishingly weak combustion rather than flame instability.

In addition, many salient features of HCCI may be observed in Figure 5 and Figure 6. For instance, both cases demonstrate that ignition occurs at the center of the combustion chamber—although this is somewhat difficult to notice in Figure 5. Another feature visible in Figure 6 is that no discernible flame front exists. Instead, the charge is consumed—albeit partially—through a series of explosions. Moreover, both cases demonstrate that combustion is "quenched" by the gas expansion rather than contact with a boundary. Finally, both Figure 5 and Figure 6 attest that HCCI combustion is very fast.

Image	Comments
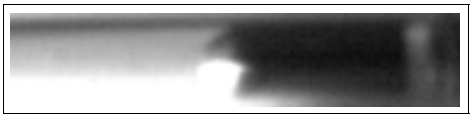	Compression stroke, $t = t_0$. Distance between piston and end plug: 1.1 mm.
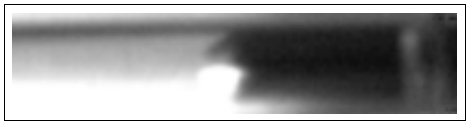	Compression stroke, $t = t_0 + 16\mu$s. Distance between piston and end plug: 0.5 mm.
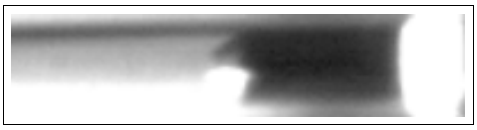	Ignition, $t = t_0 + 32\mu$s. Distance between piston and end plug: 0.3 mm.
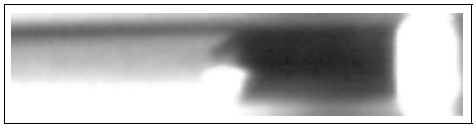	Combustion and beginning of the expansion stroke, $t = t_0 + 64\mu$s. Distance between piston and end plug: 0.5 mm.
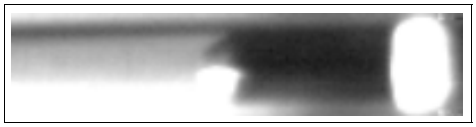	Expansion stroke, $t = t_0 + 96\mu$s. Distance between piston and end plug: 0.8 mm.
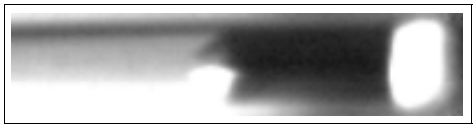	Expansion stroke, $t = t_0 + 128\mu$s. Distance between piston and end plug: 1.1 mm.
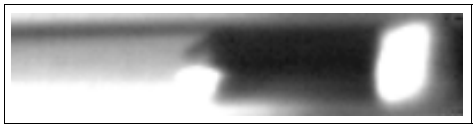	Expansion stroke, $t = t_0 + 160\mu$s. Distance between piston and end plug: 1.5 mm.
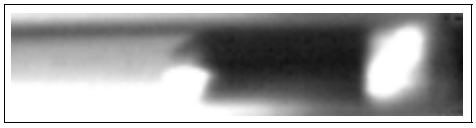	Expansion stroke, $t = t_0 + 192\mu$s. Distance between piston and end plug: 1.9 mm.
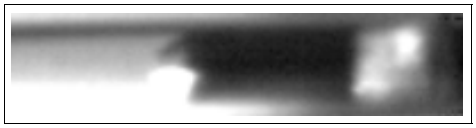	Expansion stroke, $t = t_0 + 224\mu$s. Distance between piston and end plug: 2.8 mm.
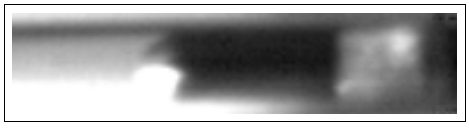	Expansion stroke, $t = t_0 + 256\mu$s. Distance between piston and end plug: 3.3 mm.
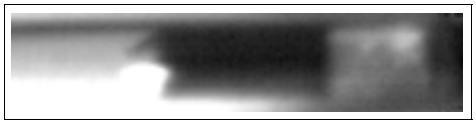	Expansion stroke and end of combustion, $t = t_0 + 288\mu$s. Distance between piston and end plug: 3.9 mm.

Figure 5. A typical sequence of images from a single-shot experiment. The fuel is n-heptane and the equivalence ratio is estimated to be 0.69. Also, the charge was initially at room temperature and pressure. Refer to Figure 4 for additional dimensions ($L_{\text{T}} \approx 57\,\text{mm}$).

Image	Comments
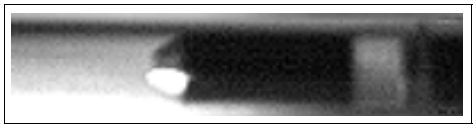	Compression stroke, $t = t_0$. Distance between piston and end plug: 1.7 mm.
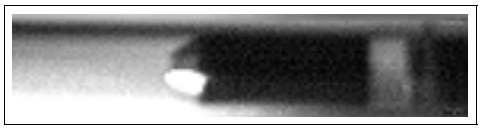	Compression stroke, $t = t_0 + 16\mu$s. Distance between piston and end plug: 1.5 mm.
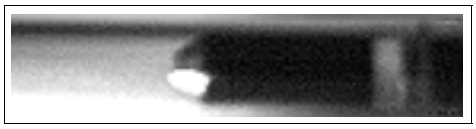	Compression stroke, $t = t_0 + 32\mu$s. Distance between piston and end plug: 0.9 mm.
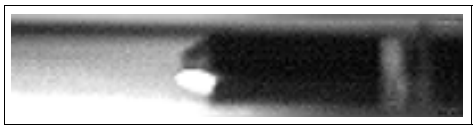	Compression stroke, $t = t_0 + 64\mu$s. Distance between piston and end plug: 0.8 mm.
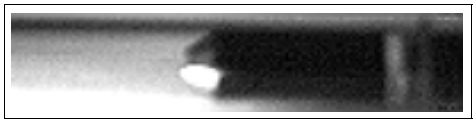	Compression stroke, $t = t_0 + 96\mu$s. Distance between piston and end plug: 0.4 mm.
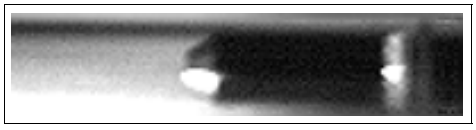	Combustion and beginning of the expansion stroke, $t = t_0 + 128\mu$s. Distance between piston and end plug: 0.7 mm.
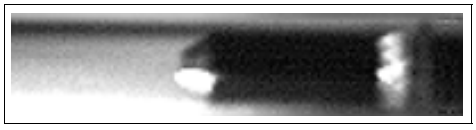	Expansion stroke, $t = t_0 + 160\mu$s. Distance between piston and end plug: 0.9 mm.
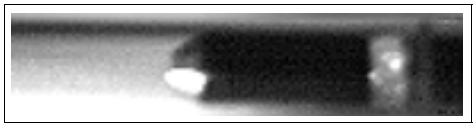	Expansion stroke, $t = t_0 + 192\mu$s. Distance between piston and end plug: 1.2 mm.
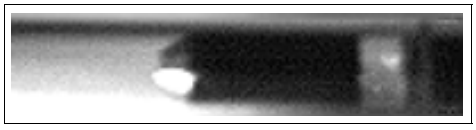	Expansion stroke, $t = t_0 + 224\mu$s. Distance between piston and end plug: 1.7 mm.
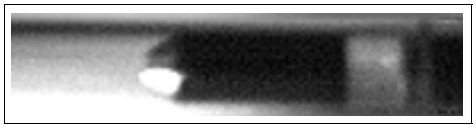	Expansion stroke, $t = t_0 + 256\mu$s. Distance between piston and end plug: 2.2 mm.
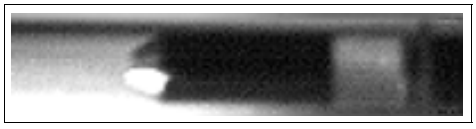	Expansion stroke and end of combustion, $t = t_0 + 288\mu$s. Distance between piston and end plug: 2.9 mm.

Figure 6. A typical sequence of images from a single-shot experiment. The fuel is n-heptane and the equivalence ratio is estimated to be 0.25. Also, the charge was initially at room temperature and pressure. Refer to Figure 4 for additional dimensions ($L_{\text{T}} \approx 57$ mm).

Modeling the Single-Shot Experiments

After establishing that HCCI *is* a viable micro-combustion scheme by conducting numerous single-shot experiments and observing ignition, the next logical step is to model these experiments. Clearly, such a model would need to incorporate both detailed chemical kinetics and free-piston dynamics. A necessary prelude to developing such a model however, is to thoroughly understand free-piston dynamics. This is accomplished by modeling the single shot experiments without combustion.

The initial model was developed by assuming that the compression was isentropic, the gas perfect, and the piston frictionless. Consequently the model consisted of a force balance and an isentropic relation. The resulting ordinary differential equation was then integrated to give the piston position and velocity versus time. Earlier, it was mentioned that the Pyrex tubes are matched to the piston such that the clearance between them is approximately $5\,\mu$m. Initially, the gas escaping through this gap, or blow-by, was neglected. It turns out however, that blow-by is significant. On the other hand, a frictionless piston was found to be an excellent assumption—due to the gas rushing through the gap.

To incorporate leakage in the single-shot model, it was necessary to simultaneously solve ordinary differential equations derived from mass, energy, and force balances. Additionally, the mass flow rate of the gas was described using one-dimensional quasi-steady compressible flow. Also, the heat transfer model developed by Aichlmayr et al. [28] was incorporated. Although heat transfer was found to negligibly affect the piston motion.

Representative results from the single-shot experiment models and comparisons to experimental data are presented in Figure 7. The significance of blow-by is evident in Figure 7(a). Specifically, it causes the position versus time profile to be asymmetrical. On the other hand, the compression stroke is virtually identical to the ideal, i.e., leakage-free, model. This result is partially explained by Figure 7(c). That is, the majority of the mass is lost when the piston is nearly stationary (Figure 7(b)) at the end of the compression stroke. Likewise, little mass is lost during the expansion stroke. Additionally, because a significant amount of mass is lost at the end of the compression stroke, the outgoing piston velocity is greatly reduced (Figure 7(b)). Another consequence of blow-by is that the overall compression ratio is exaggerated. Many other physical insights may be gleaned, but they will be presented following further refinement of the model.

Conclusions and Future Work

This paper has presented experimental evidence that HCCI is a viable micro-engine combustion scheme. Furthermore, it has been demonstrated that micro-combustion can be achieved without resorting to catalysts or external heating; thus micro-HCCI is promising. Moreover, the property that extremely lean mixtures may be ignited is preserved. In contrast, ancillary concerns such as blow-by, were demonstrated to be appreciable. Consequently further micro-engine development efforts must focus upon practical aspects. In the near term however, the HCCI combustion and free-piston interaction will be investigated in far greater detail. Additionally, the single-shot experiments will continue. They will be extended to smaller tube length experiments, i.e., approaching practical engine dimensions, testing more fuels, and chemical analysis of the products.

Acknowledgement

This project was sponsored by Honeywell International under DARPA contract No. F30602-99-C-0200. The authors would also like to thank Dr. Wei Yang and Mr. Tom Rezachek of Honeywell International for designing and providing equipment for the single-shot experiments.

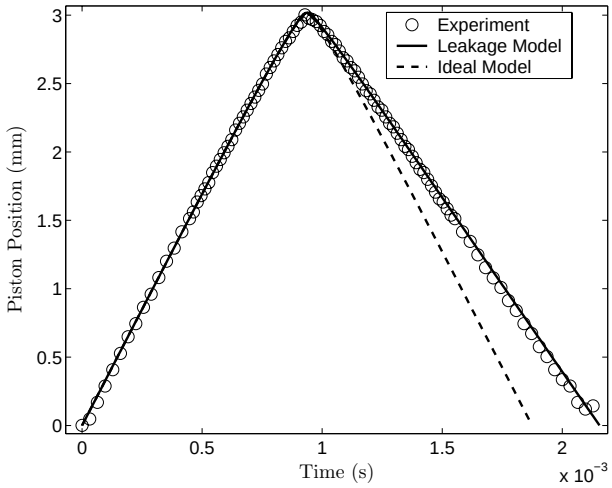

(a) Piston Position (an experimental uncertainty of 0.03 cm is omitted for clarity)

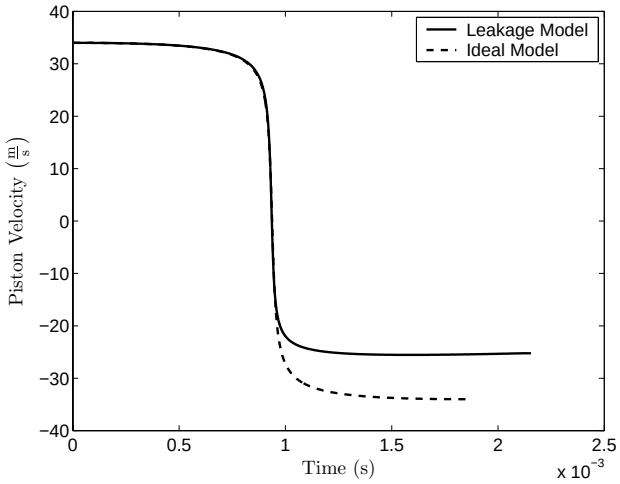

(b) Piston Velocity

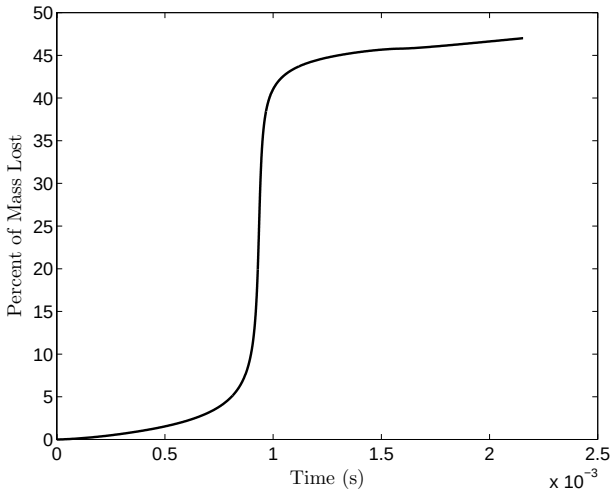

(c) Percent Mass Lost (Leakage Model)

Figure 7. Results of single-shot experiment models, $L_{\mathrm{T}} = 30\,\mathrm{mm}$, γ=1.31, and the initial velocity is $34\,\frac{\mathrm{m}}{\mathrm{s}}$.

Nomenclature

A_{B}	Bounce Piston Area $\left(\text{m}^2\right)$, Eq. (2).
A_{C}	Combustion Piston Area $\left(\text{m}^2\right)$, Eq. (2).
A_{s}	Surface area $\left(\text{m}^2\right)$, Eq. (1).
$\frac{\text{A}_{\text{s}}}{\tilde{\text{V}}}$	Surface area to volume ratio $\left(\frac{1}{\text{m}}\right)$, Eq. (1).
F_x	x-Direction force (N)
L_{T}	Initial distance between piston and tube end (mm)
m	Mass of material (kg), Eq. (1).
m_{P}	Piston Mass (kg), Eq. (2).
P_{B}	Bounce Chamber Pressure (atm), Eq. (2).
P_{C}	Combustion Chamber Pressure (atm), Eq. (2).
$\dot{Q}$	Heat transfer rate (W), Eq. (1).
$\dot{q}''$	Heat flux $\left(\frac{\text{W}}{\text{m}^2}\right)$, Eq. (1).
$\dot{q}$	Specific heat transfer rate $\left(\frac{\text{W}}{\text{kg}}\right)$, Eq. (1).
$\bar{\dot{q}}''$	Average heat flux $\left(\frac{\text{W}}{\text{m}^2}\right)$, Eq. (1).
R	Stroke-to-bore aspect ratio, unitless.
r	Volumetric compression ratio, unitless.
t	Time (s)
V_{t}	Total cylinder volume $\left(\text{mm}^3\right)$.
$\tilde{\text{V}}$	Volume $\left(\text{m}^3\right)$, Eq. (1).
x	Cartesian Coordinate
Φ	Fuel-air equivalence ratio, unitless.
γ	Specific heat ratio, unitless.
ρ	Density $\left(\frac{\text{kg}}{\text{m}^3}\right)$, Eq. (1).
$\bar{\rho}$	Average density $\left(\frac{\text{kg}}{\text{m}^3}\right)$, Eq. (1).

References

[1] Epstein, A. H., Senturia, S. D., Anathasuresh, G., Ayon, A., Breuer, K., Chen, K., Ehrich, F. E., Gauba, G., Ghodssi, R., Groshenry, C., Jacobson, S., Lang, J. H., Lin, C., Mehra, A., Miranda, J. M., Nagle, S., Orr, D. J., Piekos, E., Schmidt, M. A., Shirley, G., Spearing, M. S., Tan, C. S., Tzeng, Y., and Waitz, I. A. Power MEMS and microengines. In *Transducers '97 Chicago : digest of technical papers*, pp. 753–756. IEEE, Chicago, Ill (1997).

[2] Fernandez-Pello, C., Liepmann, D., Pisano, A., et al. MEMS rotary combustion laboratories. University of California at Berkeley Internet Document (Last loaded July 2001) (2001). URL `http://www.me.berkeley.edu/mrcl/`.

[3] Yang, W., Bonne, U., et al. MEMS free-piston knock engine. Technical Proposal, DARPA Contract F30602-99-C-0200 (1999). Honeywell Technology Center, 12001 State Highway 55, Plymouth, MN 55441.

[4] Yang, W., Bonne, U., and Johnson, B. R. Microcombustion engine/generator. U. S. Patent 6,276,313 (2001).

[5] Allen, M. et al. Research topics–miniature MEMS free-piston engine generator. Georgia Institute of Technology Internet Document (Last loaded July 2001) (2001). URL `http://comblab5.ae.gatech.edu/Minipiston/intro.htm`.

[6] Yang, W. Personal communication (2000).

[7] Waitz, I. A., Gauba, G., and Tzeng, Y. Combustors for Micro-Gas Turbine Engines. *Journal of Fluids Engineering* **120**(1) pp. 109–117 (1998).

[8] Onishi, S., Jo, S. H., Shoda, K., Jo, P. D., and Kato, S. Active thermo-atmosphere combustion (ATAC)–a new combustion process for internal combustion engines. *SAE Technical Paper 790501* (1979).

[9] Najt, P. M. and Foster, D. E. Compression-ignited homogeneous charge combustion. *SAE Technical Paper 830264* (1983).

[10] Iida, N. Combustion analysis of methanol-fueled active thermo-atmosphere combustion (ATAC) engine using a spectroscopic observation. *SAE Technical Paper 940684* (1994).

[11] Lavy, J., Duret, P., Habert, P., Esterlingot, E., and Gentili, R. Investigation on controlled auto-ignition combustion (A.T.A.C.) in two-stroke gasoline engine. In *Selected Presentations from the Second International Workshop and Thematic Network Meeting on Modernised 2/Stroke Engines*, The 2/Stroke Thematic Network Circular. Manchester, UK (1996).

[12] Gentili, R., Frigo, S., Tognotti, L., Patrice, H., and Lavy, J. Experimental study on ATAC (Active Thermo-Atmosphere Combustion) in a two-stroke gasoline engine. *SAE Technical Paper 970363* (1997).

[13] Thring, R. H. Homogeneous-charge compression ignition (HCCI) engines. *SAE Technical Paper 892068* (1989).

[14] Ryan, III, T. W. and Callahan, T. J. Homogeneous charge compression ignition of diesel fuel. *SAE Technical Paper 961160* (1996).

[15] Aoyama, T., Hattori, Y., and Mizuta, J. An experimental study on premixed-charge compression ignition gasoline engine. *SAE Technical Paper 960081* (1996).

[16] Christensen, M., Johansson, B., and Einwall, P. Homogenous charge compression ignition (HCCI) using isooctane, ethanol, and natural gas-a comparison with spark ignition operation. *SAE Technical Paper 972874* (1997).

[17] Gray, III, A. and Ryan, III, T. W. Homogeneous charge compression ignition (HCCI) of diesel fuel. *SAE Technical Paper 971676* (1997).

[18] Christensen, M. and Johansson, B. Influence of mixture quality on homogenous charge compression ignition. *SAE Technical Paper 982454* (1998).

[19] Christensen, M., Johansson, B., AmnJus, P., and Mauss, F. Supercharged homogenous charge compression ignition. *SAE Technical Paper 980787* (1998).

[20] Iwabuchi, Y., Kawai, K., Shoji, T., and Takeda, Y. Trial of new concept diesel combustion system-

premixed compression-ignited combustion-. *SAE Technical Paper 1999-01-0185* (1999).

[21] Christensen, M. and Johansson, B. Homogenous charge compression ignition with water injection. *SAE Technical Paper 1999-01-0182* (1999).

[22] Hultqvist, A., Christensen, M., Johansson, B., Franke, A., Richter, M., and Alden, M. A study of the homogeneous charge compression ignition combustion process by chemiluminescent imaging. *SAE Technical Paper 1999-01-3680* (1999).

[23] Richter, M., Franke, A., Alden, M., Hultqvist, A., and Johansson, B. Optical diagnostics applied to a naturally aspirated homogenous charge compression igntion engine. *SAE Technical Paper 1999-01-3649* (1999).

[24] Christensen, M., Hultqvist, A., and Johansson, B. Demonstrating the multi fuel capability of a homogeneous charge comression ignition engine with variable compression ratio. *SAE Technical Paper 1999-01-3679* (1999).

[25] Flowers, D., Aceves, S., Smith, R., Torres, J., Girard, J., and Dibble, R. HCCI in a CFR engine: Experiments and detailed kinetic modeling. *SAE Technical Paper 2000-01-0328* (2000).

[26] Chen, Z., Konno, M., Oguma, M., and Yani, T. Experimental study of CI natural-gas/DME homogeneous charge engine. *SAE Technical Paper 2000-01-0329* (2000).

[27] Aichlmayr, H. T., Kittelson, D. B., and Zachariah, M. R. Miniature free-piston homogeneous charge compression ignition engine concept part I: Performance estimation and design considerations unique to small dimensions (2001). Under review.

[28] Aichlmayr, H. T., Kittelson, D. B., and Zachariah, M. R. Miniature free-piston homogeneous charge compression ignition engine concept part II: Modeling HCCI combustion in small-scales with detailed homogeneous gas phase chemical kinetics (2001). Under review.

[29] Aceves, S. M., Smith, J. R., Westbrook, C. K., and Pitz, W. J. Compression ratio effect on methane HCCI combustion. *Jounal of Engineering for Gas Turbines and Power* **121**(3) pp. 569–574 (1999).

[30] Lutz, A. E., Kee, R. J., and Miller, J. A. Senkin: A fortran program for predicting homogeneous gas phase chemical kinetics with sensitivity analysis. Sandia Rep. SAND87-8248, Sandia National Laboratory (1988).

[31] Van Blarigan, P., Paradiso, N., and Goldsborough, S. S. Homogeneous charge compression ignition with a free piston: A new approach to ideal Otto cycle performance. *SAE Technical Paper 982484* (1998).

[32] Goldsborough, S. S. and Van Blarigan, P. A numerical study of a free piston ic engine operating on homogeneous charge compression ignition combustion. *SAE Technical Paper 990619* (1999).

[33] Van Blarigan, P. Free-piston engine. U. S. Patent 6,199,519 (2001).

[34] Achten, P. A. J. A review of free piston engine concepts. *SAE Technical Paper 941776* (1994).